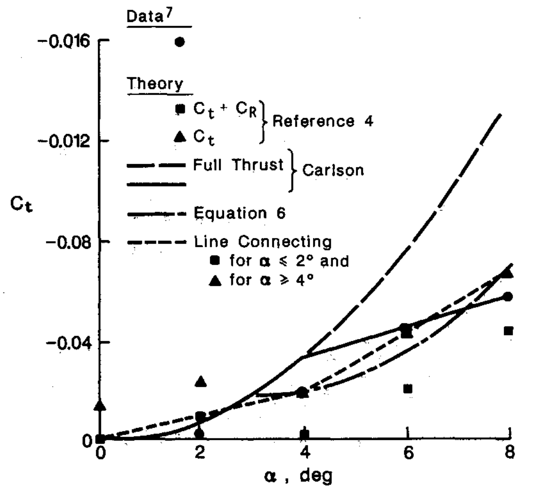

Fig. 4 Variation of leading-edge suction with angle of attack for an NACA 64A009 airfoil. $M=0.4$, $Re=0.86\times10^6$.

the values of α_s and c_t are approximately the same at Reynolds numbers equal to 5.8 and 0.58×10^6. Figure 2 shows the effect of thickness on c_t at $\alpha=\alpha_s$. Again it is seen that the sum of c_t and c_R is approximately zero for all thickness ratios examined. This is precisely Kulfan's concept. The accuracy of the concept for thick airfoils is slightly less than that for thin airfoils.

The camber effect is illustrated in Fig. 3 for four NACA four-digit airfoils. It is seen that at α_s, c_t is greater than c_R. This is due to the pressure thrust generated on the forward camber (to be called the camber thrust in the following). To remove the camber thrust in performing the pressure integration, the slope of the upper airfoil surface is reduced by the local mean line slope and that of the lower surface is increased by it. The results indicated in Fig. 3 by hexagonal symbols show that Kulfan's concept is still reasonable if camber thrust is removed from the net suction. In applications in thin airfoil or wing theory, this is usually true, because c_t as given by Eq. (3) does not contain the contribution of camber thrust.

Table 1 shows the difference in α_s predicted by the code of Ref. 4 and Eq. (5) the thin airfoil theory of Eq. (5). It is seen that α_s calculated with Eq. (5) is reasonable only if the camber is small.

To find out whether Kulfan's method is realistic for estimation of attainable thrust, theoretical c_t is compared with experimental data for an NACA 64A009 airfoil in Fig. 4. The circles represent the experimental data and the solid line is obtained by Carlson and Mack's empirical method. It is seen that in addition to the solid line, the short-dash curve matches the experimental results well. The short-dash curve is obtained by connecting the calculated results for c_t at $\alpha\geq4$ deg (triangles) and for c_t+c_R at $\alpha\leq2$ deg (squares). The squares represent the suction obtained by integrating the calculated viscous pressure over the region forward of the separation bubble. These calculated results underpredict the net leading-edge suction for $\alpha>2$ deg. Since the code of Ref. 4 cannot predict the size of the separation bubble, one possible explanation is that additional suction is present between the bubble and the maximum thickness location and is not included in the calculation. It is also seen that the short-dash curve, which represents the results obtained from the code of Ref. 4, agrees well with those based on Kulfan's method [Eq. (6)]. There is a definite reduction of c_t for any α greater than α_s (which is about 3 deg by Kulfan's method and 4 deg by Carlson and Mack's method) as compared to the theoretical full suction coefficient. This two-dimensional airfoil result is consistent with the three-dimensional concept that the leading-edge vortex on a wing with a round-nosed airfoil, once formed, would be of reduced strength relative to a thin sharp wing.

Conclusions

Kulfan assumed that the angle of attack for initial vortex separation on a slender wing with rounded leading edges could be obtained by equating the leading-edge suction and nose drag coefficients. This assumption has been examined and was shown to predict reasonably well the initial angle of attack at which laminar separation occurs near the airfoil nose. The assumption was shown to be slightly less accurate for thick or cambered airfoils. Attainable leading-edge suction estimated by Kulfan's method appeared to agree well with that obtained from an airfoil aerodynamics code and experimental data for a NACA 64A009 airfoil at $M=0.4$ and $Re=0.86\times10^6$.

Acknowledgment

This work was supported by NASA Grant NSG-1629.

References

[1]Carlson, H. W. and Mack, R. J., "Studies of Leading-Edge Thrust Phenomena," *Journal of Aircraft,* Vol. 17, Dec. 1980, pp. 890–897.

[2]Kulfan, R. M., "Wing Airfoil Shape Effects on the Development of Leading-Edge Vortices," AIAA Paper 79-1675, Aug. 1979.

[3]Kulfan, R. M., "Wing Geometry Effects on Leading Edge Vortices," AIAA Paper 79-1872, Aug. 1979.

[4]Stevens, W. A., Goradia, S. H., and Braden, J.A., "Mathematical Model for Two-Dimensional Multi-Component Airfoils in Viscous Flow," NASA CR-1843, July 1971.

[5]Robinson, A. and Laurmann, J. A., *Wing Theory,* Cambridge University Press, New York, 1956.

[6]McCullough, G. B. and Gault, D. E., "Examples of Three Representative Types of Airfoil-Section Stall at Low Speed," NACA TN 2502, Sept. 1951.

[7]Daley, B.N. and Dick, R.S., "Effect of Thickness, Camber and Thickness Distribution on Airfoil Characteristics at Mach Numbers up to 1.0," NACA TN 3607, 1956.

Residual Stresses in 2024-T81 Aluminum Using Caustics and Moiré Interferometry

Basil P. Leftheris* and Robert Schwarz†
Grumman Corporate Research Center
Bethpage, New York

Introduction

CRACK growth information is important in estimating fatigue life in aircraft structures. The interaction between existing residual stresses in aluminum alloy sheet stock and residual stresses induced by cold-working the holes is difficult to evaluate analytically, mainly because existing residual stresses are not clearly defined. However, such cases can be evaluated experimentally with fatigue specimens under cyclic loading by observing the changes in the stress intensity factor K_I during crack growth.

The method of caustics, also known as the shadow method, can be used during cyclic fatigue testing, without interrupting the test, to evaluate the stress intensity factors. We use the method of caustics to evaluate the behavior of 2024-T81 aluminum alloy sheet (0.125 in. thick) in longitudinal and long

Received Sept. 8, 1986; revision received Jan. 6, 1987.

*Principal Investigator, Senior Staff Scientist. Member AIAA.
†Engineering Specialist, Test Operations.

transverse directions. In addition, the strain distributions in specimens with open holes and with cold-worked holes were obtained using the method of moiré interferometry.

This Note is an interim publication of our work on the effects of residual stresses. A full report is in preparation.

Test Description

The crack growth tests were carried out under constant amplitude cyclic loading with $R=0.1$. Specimens with cold-worked holes were subjected to variations of frequency of loading and maximum load to show whether crack growth was sensitive to these changes.

The specimens used in our tests were 1 in. wide and 5 in. long with 0.190 in. holes. One side was polished to improve reflectivity, as required for caustics, and the other was instrumented with a 500 line/in. ruling. Displacement measurements were obtained with moiré interferometry using spatial filtering that produces an effective ruling of 2540 lines/in.

Caustics of the crack tip region were obtained using a pulsed laser synchronized with the loading controls and the camera to obtain caustics at near maximum load. The caustics were projected on a screen 10 ft away from the specimen surface. The initial curve size was about 0.01 in.

Results and Discussion

Aluminum alloy specimens were tested in a special setup that allowed the recording of caustics[1] during cyclic fatigue testing. Specimens 54 and 55 were loaded at 15.2 ksi in longitudinal (L) and long transverse (LT) directions, respectively. The crack growth results are shown in Fig. 1. The number of cycles required to grow the crack in the LT direction is approximately 2.5 times that required for the L direction. Experimental results show that the crack growth rates should be about the same.[2]

The corresponding stress intensity factor K_I values evaluated from the caustics records obtained during cycling are shown in Fig. 2. The K_I values obtained from the Bowie theoretical[3] solution of the specimen without residual stresses is also plotted for comparison. In Fig. 2, the test results obtained with the L specimen are in close agreement with the theoretical value, as expected for open holes without cold work. By comparison, the test results which were obtained with the LT specimen are below the expected theoretical values, a characteristic usually expected from cold-worked holes.[4] Since the holes are not cold-worked, the advantage indicated in fatigue enhancement results from residual stresses in the material.

In another set of tests, we cold-worked the hole using the sleeve method. The results of crack growth are shown in Fig. 3. Specimen 43 is loaded in the LT direction and 44 in the L direction. Since material residual stresses are possibly due to rolling and long grain configuration, we used specimen 45 machined from 0.250 in. thick plate. Small changes in cycling frequency and maximum load were introduced to influence the rate of crack growth. The results, however, show that the crack growth required in the LT direction was again approximately 2.5 times the number of cycles required for the L direction. Again, based on theoretical considerations, the crack growth rates should have been the same.

It was becoming obvious that 2024-T81 had directional properties which could not be explained by the differences of yield strength (i.e., the stress-strain in the elastic and plastic regions are almost the same in the LT and L directions). To evaluate this directionality issue further, a number of specimens of 2024-T81, $4\times4\times0.125$ in. (sheet stock) were prepared with moiré grilles. The holes were cold-worked as before, and the strains were evaluated using moiré in-

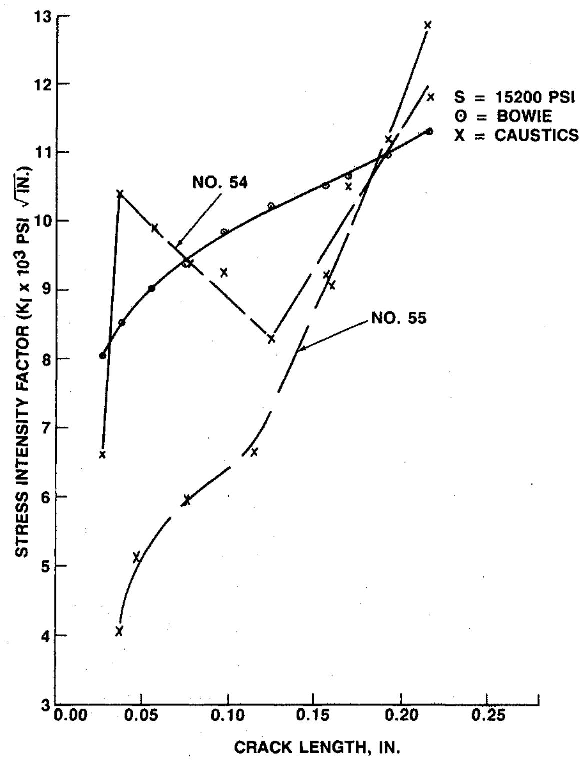

Fig. 2 Stress intensity factor K_I for 2024-T81 aluminum: specimens 54 and 55 loaded in L and LT directions, respectively.

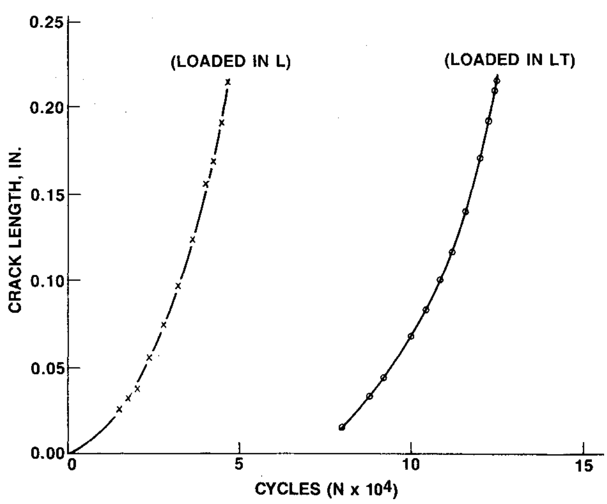

Fig. 1 Crack growth for 2024-T81 aluminum.

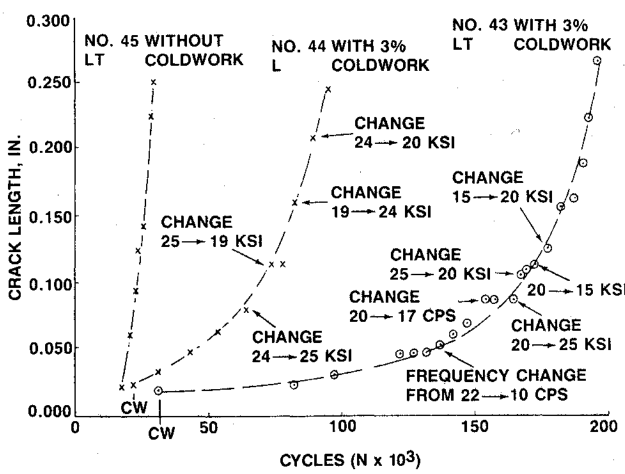

Fig. 3 Comparison of crack growth in specimens of 2024-T81 aluminum.

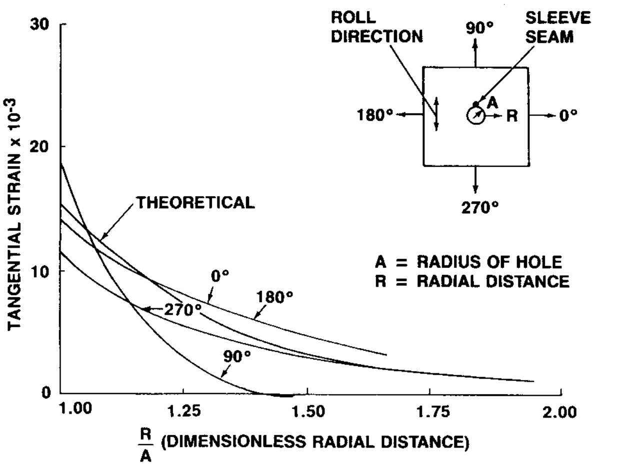

Fig. 4 Distribution of tangential strain specimen 63 hole cold-worked with sleeve method obtained with moiré interferometry (2024-T81 aluminum).

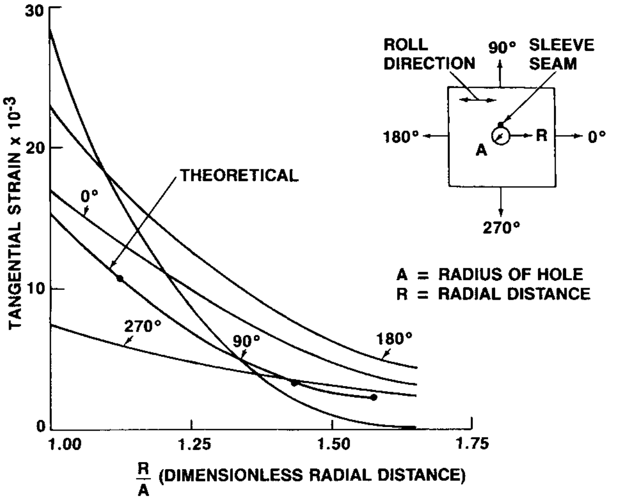

Fig. 5 Distribution of tangential strain, specimen 64 hole cold-worked with sleeve method obtained with moiré interferometry (2024-T81 aluminum).

terferometry.[1] The results are shown in Figs. 4 and 5. The specimen in the LT direction (Fig. 5) has higher fatigue enhancement than the specimen in the L direction (Fig. 4), which agrees with crack growth results (Fig. 3). This is an indication that the material has residual strains other than those generated by cold work.

Results with specimens that did not display any differences between LT and L directions show: 1) the same crack growth rates and 2) the same distribution of strains.

What is important, however, is that the strain distributions are not axisymmetric. At 90 deg where the sleeve seam is positioned, there is a sector where the residual strains are very low. The strain distribution for the same cold work (i.e., 3%) in the hole was calculated using a finite-element method. The results are included in Figs. 4 and 5. Comparison of theoretical results with experimental observations indicate that the finite-element axisymmetric model will not always be in agreement with tests results: the difference is especially large for radial strains.

Since our 2024-T81 specimens were made of 0.125 in. sheet stock that included stress relief by stretching, we compared their behavior with similar moiré interferometry tests of $5 \times 5 \times 0.250$ in. plates made of 2024-T3 cold-worked with the stress wave riveter. The results are shown in Fig. 6. The uniform strain distribution in Fig. 6 is the result of the

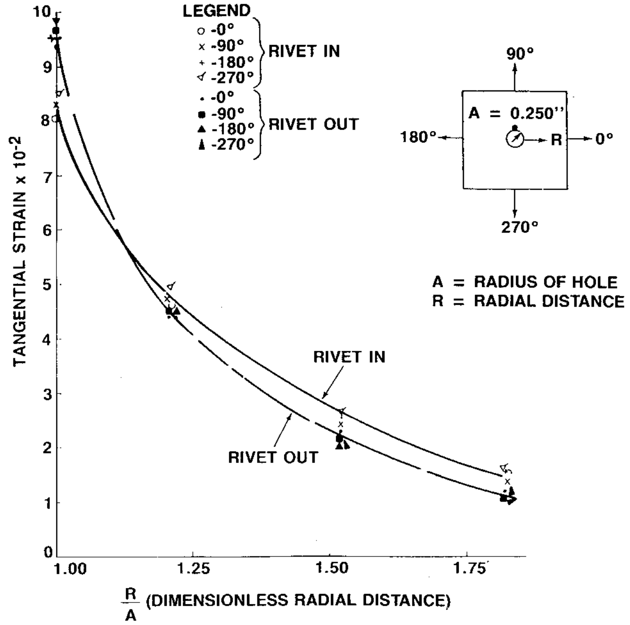

Fig. 6 Distribution of tangential strains obtained with moiré interferometry, hole cold worked with stress wave riveter with 6% permanent set (2024-T3 aluminum).

uniform radial expansion process, combined with the absence of residual stresses in the material.

Conclusions

Aluminum 2024-T81 has an unpredictable fatigue behavior attributable to the residual stresses in the material. From the limited number (10) of specimens tested, a 2.5 times advantage in fatigue life was evident for specimens loaded in the long transverse over the longitudinal direction. The advantage of the LT direction was maintained in specimens with cold-worked holes. However, some specimens, from different material lots, showed no differences in fatigue life between the LT and L directions. This indicated that residual stresses in sheets of 2024-T81 are not uniform and, hence, not predictable.

Our work also showed that the sleeve method of cold-working has an area sector spreading radially out from the sleeve seam, where the strains are near zero after cold work. This is an indication that the strain distribution around the hole is not axisymmetric, and moiré interferometry measurements cannot be compared with finite-element axisymmetric models. Furthermore, if a crack grows where the sleeve seam is positioned, fatigue enhancement may not occur from the cold-work process.

By comparison, the stress wave riveter provides more uniform radial expansion using the rivet as the tool to do the cold work instead of the mandrel and sleeve, and produces the desired axisymmetric fatigue life enhancement.

References

[1]Kobayashi, A.S. (ed.), *Handbook of Experimental Mechanics,* Society of Experimental Mechanics, Bethel, CT, 1986.

[2]Gallagher, J. (ed.), *Damage Tolerant Design Handbook*, Metals and Ceramics Information Center, Battelle Columbus Laboratories, Columbus, OH, Vol. 3, 1983, Chap. 7, pp. 161–181.

[3]Bowie, D.L., "Analysis of an Infinite Plate Containing Radial Cracks, Originating From the Boundary of an Internal Hole," *Journal of Mathematics and Physics,* Vol. 35, 1956, pp. 60–71.

[4]Cathey, W.H. and Grandt, A.F. Jr., "Fracture Mechanics Consideration of Residual Stresses Introduced by Cold Working Fastener Holes," *Journal of Engineering Materials Technology,* Vol. 102, 1980, pp. 85–90.